第 43 卷 第 21 期/2023 年 11 月/光学学报 研究论文

光学学报

基于过焦扫描光学显微镜的光学元件亚表面缺陷检测方法

王娜[1,2]，刘立拓[2*]，宋晓娇[2]，王德钊[2,3]，王盛阳[2,4]，李冠楠[2]，周维虎[1,2,3,4**]

[1]合肥工业大学仪器科学与光电工程学院，安徽 合肥，230009；

[2]中国科学院微电子研究所光电中心，北京 100029；

[3]长春理工大学光电工程学院，吉林 长春，130022；

[4]北京航空航天大学仪器科学与光学工程学院，北京 100191

摘要 微/纳米尺度亚表面缺陷会降低光学元件等透明样品的物理特性，严重影响光学及半导体领域加工制造技术的发展。为了快速、无损检测透明样品亚表面缺陷，本文针对光学元件亚表面内微米量级缺陷的检测需求，提出了一种基于过焦扫描光学显微镜（TSOM）的检测方法。利用可见光光源显微镜和精密位移台，沿光轴对亚表面缺陷进行扫描，得到亚表面缺陷的一系列光学图像。将采集到的图像按照空间位置进行堆叠，生成 TSOM 图像。通过获得所测特征的最大灰度值来获得亚表面缺陷的定位信息。提出方法对 2000 μm 深亚表面缺陷的定位相对标准差达到 0.12%。该研究为透明样品亚表面缺陷检测及其深度定位提供了一种新方法。

关键词 亚表面缺陷；缺陷检测；过焦扫描光学显微镜；深度定位

中图分类号 O439 **文献标志码** A **DOI**：10.3788/AOS230677

1 引 言

随着国内外光学、半导体领域技术的蓬勃发展，高精密光学玻璃等光滑表面的透明器件广泛应用于科技、半导体领域以及人们的日常生活中，人们对其质量要求也越来越高[1]。石英、K9 等光学玻璃是制备高能激光透镜、精密光学棱镜/透镜、光刻掩模板等光学元件的重要材料[2]。光学玻璃在研磨和抛光过程中，由于其高强度和低断裂韧性，不可避免地在亚表面产生大量结构性缺陷，包括划痕、麻点、气泡、污染颗粒、微裂纹等[3]。亚表面缺陷会降低光学元件的镀膜质量、传输性能、损伤阈值等，从而严重影响光学系统的成像质量和系统稳定性[3]。正是由于光学元件中亚表面缺陷的种种危害，在光学元件加工制备后，首先需要对元件的缺陷进行检测[4]。如何高精度检测透明光学元件的亚表面缺陷，并为透明光学元件的高精度制备提供关键参数，成为光学检测领域亟须解决的难题[5]。

目前，光学元件的亚表面缺陷检测技术处于发展阶段，尚不成熟[6]，现有检测技术主要包括破坏性和非破坏性两种技术[7]。破坏性检测技术是通过化学腐蚀、抛光或刻蚀的方法去除元件表面抛光沉积层，使亚表面缺陷暴露出来，进行显微检测。破坏性的检测技术操作简单，可以直观、有效地观察检测结果，但是会使测试缺陷与实际缺陷存在差异[8]。因此，现有的亚表面缺陷检测技术主要围绕非破坏性的检测技术展开研究。非破坏性的检测技术主要包括全内反射显微（TIRM）技术[9-10]、光学相干层析（OCT）技术[11-14]、激光共聚焦扫描显微（CLSM）技术等[15]。经过分析对比，这些检测技术不能同时兼顾分辨率和检测速度。

过焦扫描光学显微镜（TSOM）是一种基于模型的光学计算成像方法[16]，能够实现非接触、无损和快速测量三维纳米结构[17]。TSOM 具有灵敏度高、硬件系统简单、对纳米量级尺寸变化敏感、不受光学衍射极限限制、可在线检测等优势[18-19]。TSOM 已应用于晶圆表面的缺陷检测[20]、晶圆 Si 线线宽的检测[21]、三维结构的纳米尺寸测量和分析等[22]。本文对 TSOM 检测光学元件亚表面缺陷的新方法进行探索研究。

2 TSOM 检测系统及样品加工

2.1 TSOM 检测系统

本文的 TSOM 检测系统如图 1 所示。卤素灯出射的光经过分束镜和显微物镜照射到亚表面，当亚表面存在缺陷时会对入射光产生散射，散射光经过物镜成像到探测器 CCD 靶面上，进行图像采集。本系统基

收稿日期：2023-03-14；**修回日期**：2023-04-25；**录用日期**：2023-05-31；**网络首发日期**：2023-06-28

基金项目：国家重点研发计划（2020YFB2007502）

通信作者：*liulituo@ime.ac.cn；**zhouweihu@ime.ac.cn

于传统的光学显微镜，通过高精度压电陶瓷位移台控制样品的Z向移动，移动定位精度为1 nm。沿光轴对亚表面缺陷进行扫描，获取沿Z方向（光场传播方向）通过焦点（从焦点上方到焦点下方）一定范围内离焦位置的一组光学图像，并将采集到的图像按照空间位置进行堆叠[23]，形成图像立方体（TSOM cube）。取沿Z方向的TSOM立方体截面，生成TSOM图像，通过数据分析算法能够获取微米和纳米量级结构的三维信息（即尺寸、形状和位置）[16]，通过获得所检测特征的最大灰度值来定位目标。TSOM检测使用科勒照明系统，TSOM的成像系统结构形式与明场显微镜相同。

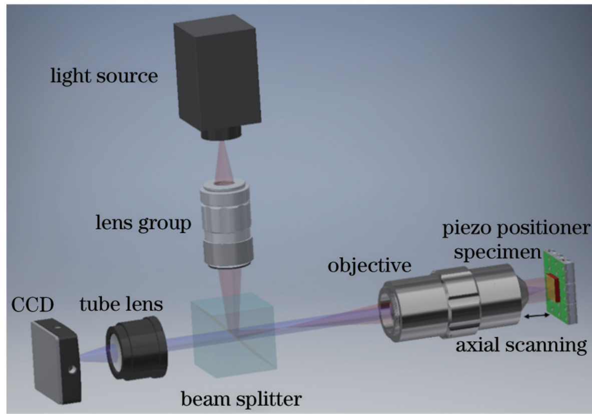

图1 TSOM检测系统示意图

Fig. 1 Schematic diagram of TSOM detection system

2.2 样品制备

1）飞秒激光加工

飞秒激光具有持续时间短、瞬时功率高、聚焦直径小、操作简单灵活等特点，可用于激光内雕，本文使用飞秒激光加工亚表面缺陷。飞秒激光加工装置实物图如图2所示，其激光波长为343 nm，激光脉宽为180 fs，最高单脉冲能量可达1.5 mJ，平均功率为6 W，重复频率为30 kHz，焦距为20 mm，加工范围为12 mm×12 mm，加工精度为5 μm。

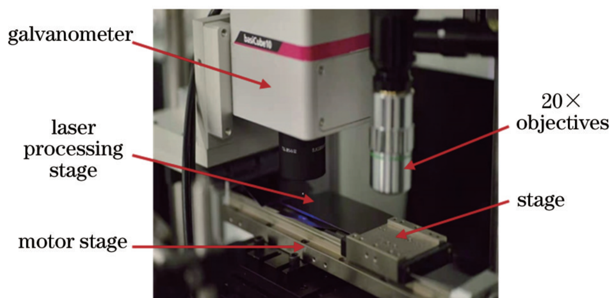

图2 飞秒激光加工装置

Fig. 2 Femtosecond laser processing device

经过大量实验分析，发现波长为343 nm的飞秒激光在石英玻璃内部加工亚表面缺陷时，石英玻璃表面会出现光致发光现象，产生蓝光，出现荧光效应，无法在样品表面以下较深的深度加工出缺陷。在K9玻璃内部可以加工出亚表面缺陷，但是损伤区域较深，出现拖尾现象，如图3所示。经过调研，选择了玻璃3D微加工的方式加工实验所需的样品。

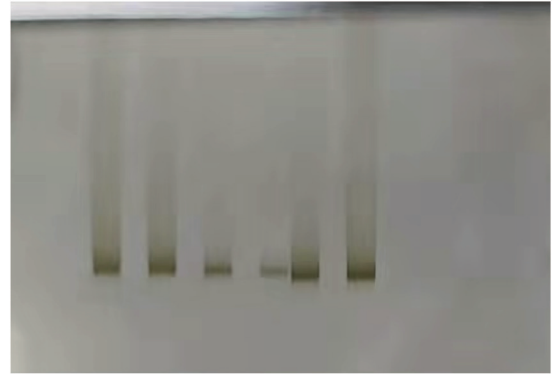

图3 飞秒激光加工K9玻璃内部损伤图

Fig. 3 Internal damage diagram of K9 glass processed by femtosecond laser

2）玻璃3D刻蚀微加工

本文采用的另一种加工缺陷的方法是3D刻蚀微加工。首先用激光对石英玻璃进行改性，然后用刻蚀的方式将改性部分的玻璃腐蚀掉，形成结构缺陷，然后对缺陷深度进行测试定位。缺陷加工时是从玻璃前表面开始，经过玻璃3D微加工后，形成从玻璃前表面开始往里延伸的长条状缺陷，如图4所示。TSOM测试时是从样品的上表面进行测试，缺陷大小约为66 μm。

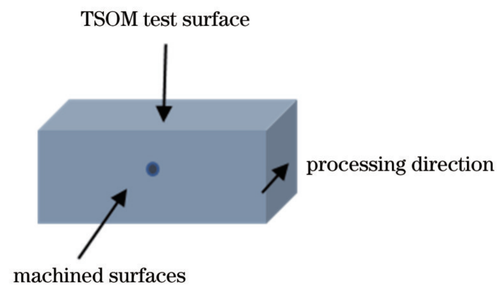

图4 样品加工示意图

Fig. 4 Schematic of sample processing

3 TSOM实验结果与分析

3.1 飞秒激光加工样品测试结果分析

测试飞秒激光加工样品亚表面缺陷时，显微镜的放大倍率为60×，数值孔径（NA）为0.75，折射率n为1.46。对飞秒激光加工的样品沿Z轴进行TSOM扫描，步长为2 μm，Z轴每移动2 μm后相机采集一幅图，移动范围为60 μm，移动范围包括缺陷散焦到聚焦再到散焦的过程，并对扫描后构建的数据立方进行处理，得到二维xz截面图，灰度最大位置则为缺陷位置，结果如图5所示。

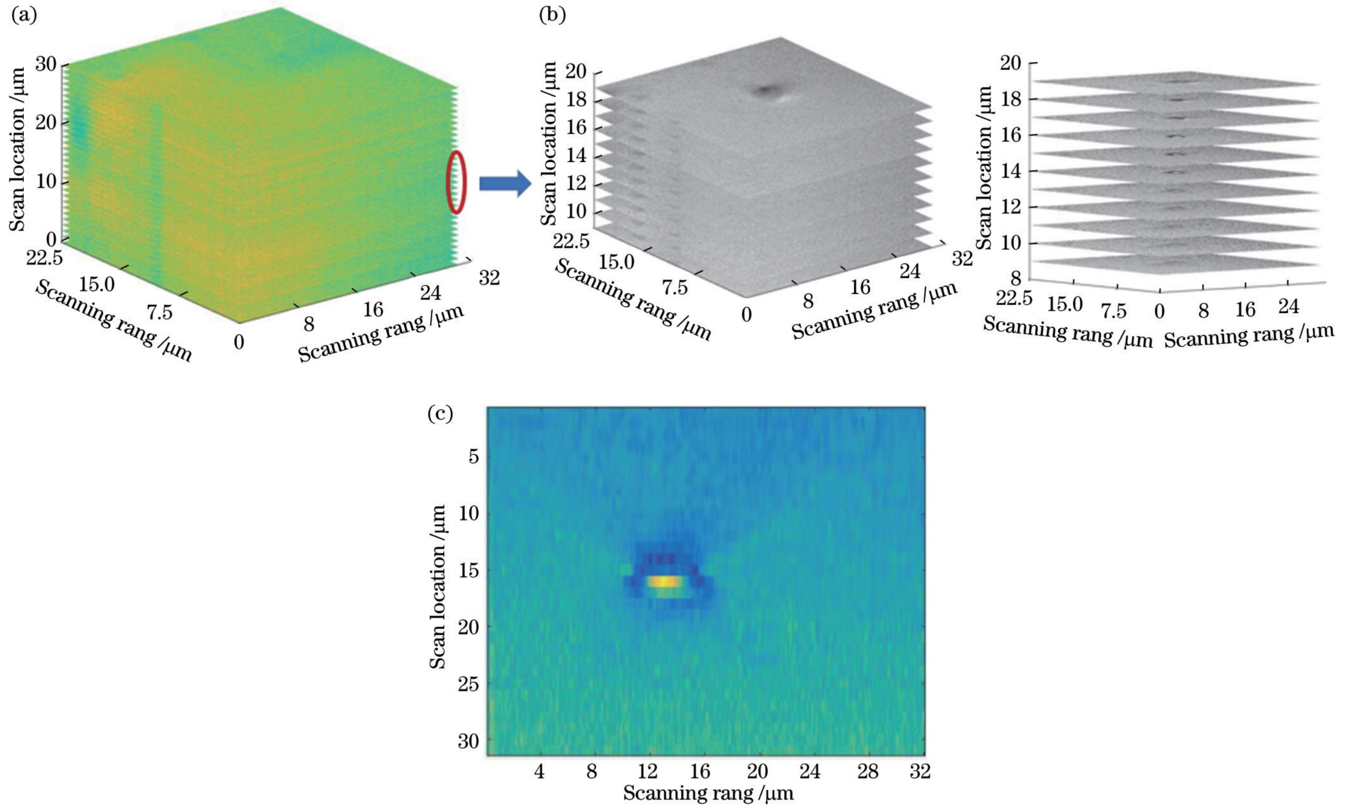

图5 飞秒激光加工样品亚表面缺陷的TSOM扫描图。(a)TSOM扫描的数据立方;(b)数据立方图的局部放大;(c)TSOM数据立方截面图

Fig. 5 TSOM scanning image of subsurface defects of femtosecond laser processing sample. (a) Data cube of TSOM scanning; (b) partial magnification of data cube; (c) TSOM data cubic cross section

TSOM测试数据立方如图5(a)所示,由于数据立方堆叠在一起时,测试结果不明显,因此将中间10幅图进行放大,如图5(b)所示,可以观察到TSOM扫描亚表面缺陷时的离焦情况。TSOM数据立方的截面结果如图5(c)所示,通过截面图可以清楚地显示TSOM扫描时的离焦情况。经过TSOM图像灰度分析,灰度最大的位置为表面以下约2 μm处,因此缺陷在表面以下约2 μm处。本样品加工误差大,同时测试未结合高精度位移台,因此样品测试结果精度不高,但仍说明了TSOM方法可以用来测试、定位微米量级亚表面缺陷。

3.2 3D微加工样品测试结果分析

为进一步提高亚表面缺陷的定位精度,需结合高精度位移台进行样品扫描。对3D微加工的样品缺陷进行TSOM扫描,步长为1 μm。由于缺陷深度超过压电陶瓷控制位移台的量程范围,因此样品表面到缺陷的距离,使用机械调节旋钮进行定位,之后再使用压电陶瓷高精度控制位移台进行TSOM扫描,在240 μm的扫描范围内建立数据立方并对数据立方进行处理,结果如图6所示。

3.3 3D微加工样品实验结果分析

显微镜测试亚表面缺陷时,缺陷会对入射光产生散射,散射光通过成像系统成像到探测器CCD上。根据菲涅耳理论,光作用到不同折射率材料上时反射和折射存在差异。为了得到实际缺陷深度,需要考虑折射率的影响进行补偿,实现校正,如图7所示。

图7中F为物镜的焦距,D为物镜的孔径,θ_1和θ_2分别为散射光不发生折射和发生折射时与法线的夹角,线段AB的长度为机械平台移动的距离,线段AC的长度为光经过玻璃折射后缺陷的实际深度。根据折射定理,经过分析推导,TSOM扫描时,亚表面缺陷的深度计算公式为

$$L=\Delta S\sqrt{n^2+\left(n^2-1\right)\frac{NA^2}{1-NA^2}}\,,\tag{1}$$

式中:L为亚表面缺陷的实际深度;ΔS为机械平台移动距离;NA为物镜的数值孔径;n为玻璃的折射率。通过折射率的补偿矫正,可进一步提高亚表面缺陷的深度定位精度。

测试3D微加工样品亚表面缺陷时,显微镜的放大倍率为40×,NA为0.6,折射率n为1.47,缺陷半径为33 μm,TSOM多次扫描经过折射率补偿后,测试光强最大位置的结果如表1所示。经过多次测量,缺陷深度的平均值为1967.3 μm,标准偏差为2.4 μm,相对标准偏差为0.12%。

为了验证缺陷的深度,使用实验室的远心成像系

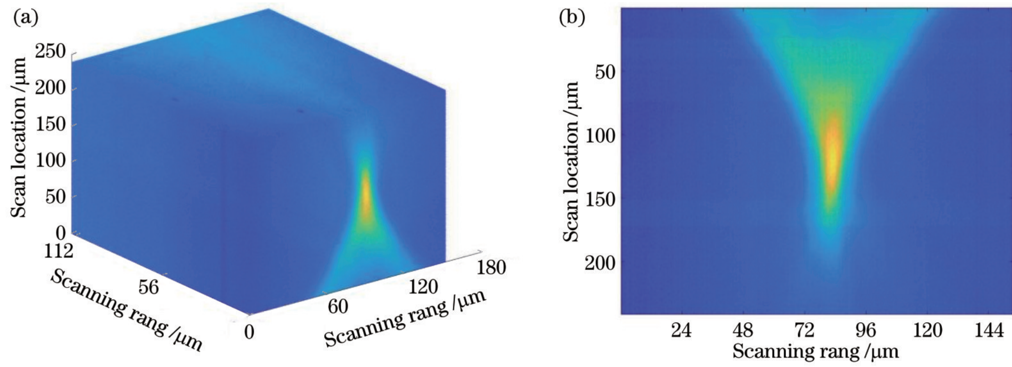

图 6 3D 微加工样品亚表面缺陷 TSOM 扫描图。(a)TSOM 扫描的数据立方;(b)TSOM 数据立方截面图

Fig. 6 TSOM scanning image of subsurface defects of 3D micromachined sample. (a) Data cube of TSOM scanning; (b) TSOM data cubic cross section

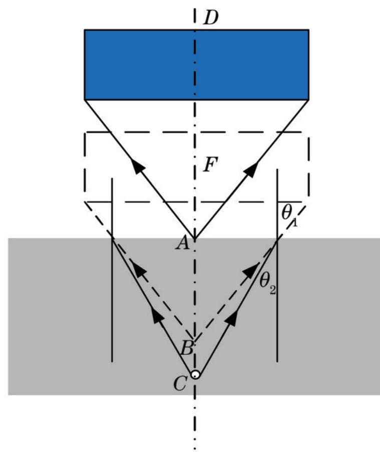

图 7 光作用到不同折射率材料上的折反射示意图

Fig. 7 Schematic diagram of refraction and reflection of light acting on materials with different refractive indices

表 1 3D 微加工样品亚表面缺陷 TSOM 多次测试结果

Table 1 Multiple TSOM test results of subsurface defects of 3D micromachined samples

Number of scans	TSOM scan depth /μm	Number of scans	TSOM scan depth /μm
1	1963.1	9	1963.1
2	1966.1	10	1969.0
3	1967.1	11	1966.1
4	1967.5	12	1964.6
5	1967.5	13	1969.0
6	1968.3	14	1970.5
7	1966.8	15	1971.9
8	1969.0	16	1967.5

统从样品表面测量缺陷中心位置距样品边缘的距离,其距离约为 2000 μm,如图 8 所示。这一结果与 TSOM 的测试结果相差 32.7 μm。

为了进一步确定缺陷距样品表面的深度,中国计量科学研究院使用超景深数码显微镜进行计量,测试方法也是从样品表面测量缺陷中心距样品边缘的距离,测试结果为 2002.1 μm,结果如图 9 所示,该结果与

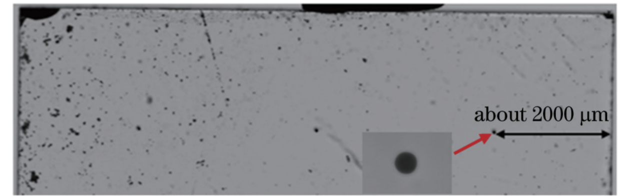

图 8 3D 微加工样品表面测试图

Fig. 8 Surface test diagram of 3D micromachined sample

中国计量科学研究院

报告编号 QYnm2022-00965

测 试 结 果

编 号	标称值(μm)	测量值(μm)
20220712	2000	2002.1

注:测量位置为客户指定位置。

图 9 中国计量科学研究院测试 3D 微加工样品表面缺陷距边缘的距离结果

Fig. 9 Results of distance between surface defects and edges of 3D micromachined samples tested by National Institute of Metrology, China

TSOM 测试结果相差 34.8 μm。

经过对 TSOM 多次扫描的缺陷深度结果进行分析,其结果与远心成像系统以及中国计量科学研究院的测试结果约有一个缺陷半径的误差。为了分析这一误差,确定 TSOM 扫描最大光强对应的位置,本文进行了时域有限差分(FDTD)仿真分析。

本文测试的 3D 微加工亚表面缺陷直径约为 66 μm,为了确定缺陷的光散射特征,使用 FDTD 仿真观察距离缺陷中心不同高度位置的光强分布。由于计算机性能受限,无法将仿真物体尺寸设置得与实验中测试的样品尺寸一致。仿真时基底玻璃尺寸为 140 μm×40 μm×240 μm,缺陷直径为 66 μm,深度为 87 μm,y 方向为周期性边界条件,其余为吸收边界,入

射光波长为532 nm。监测距离缺陷中心不同高度位置的光强变化。缺陷中心为0 μm，大于0 μm代表缺陷中心以上高度位置，小于0 μm代表缺陷中心以下高度位置，监测范围为±35 μm，监测步长为5 μm，缺陷表面±33 μm处的仿真结果如图10所示。从图10可以看出，缺陷的上表面位置处，散射光强最大。因此，TSOM扫描缺陷最大光强对应的位置是平行光轴的半径与切线a相交的p点，如图11所示。图11中，o为缺陷中心，r为平行于光轴的半径，切线a与半径r相切于p点。

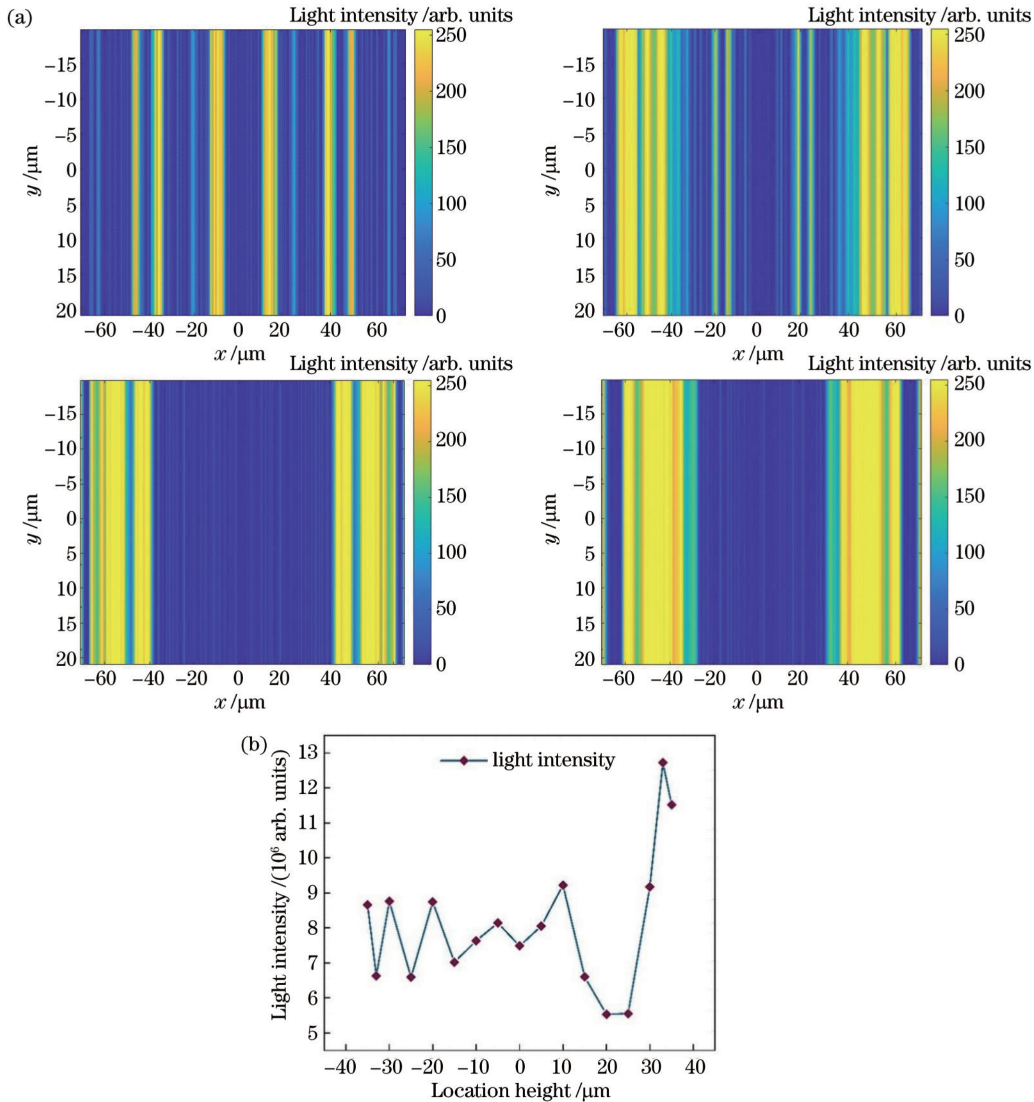

图10　FDTD仿真距离亚表面缺陷中心不同高度位置的光强。(a)35、33、0、−33 μm高度处的仿真光强分布；(b)不同高度的仿真光强变化趋势

Fig. 10　FDTD simulated light intensities at different location heights from subsurface defect center. (a) Simulated light intensity distributions at location heights of 35, 33, 0, and −33 μm; (b) simulated light intensity change trend at different location heights

当缺陷尺寸较大、缺陷存在体积效应、光照射到缺陷上时，其散射光分布与缺陷的形状、大小等参数相关，过焦扫描的灰度最大位置位于缺陷表面。因此，为得到缺陷中心到样品表面的深度，需要加上缺陷半径。将表1中TSOM扫描深度加上缺陷半径大小进行修正，从而得到缺陷中心到样品表面的深度，结果如表2所示。

表2中，缺陷深度的平均值为2000.3 μm，标准偏差为2.4 μm，相对标准偏差为0.12%，中国计量科学研究院的测试结果与修正后的缺陷深度存在1.8 μm的偏差。超景深数码显微镜测量缺陷中心距样品边缘的距离时，缺陷中心通过拟合确定，但是样品存在边缘效应，边缘不是锐利的分界线，而是清晰度逐渐变化，通过人眼确定样品边缘存在微米量级偏差。

4　结　论

经过实验验证，TSOM的方法可用于透明玻璃内微米量级亚表面缺陷的检测，并定位亚表面缺陷的深度，相对标准差可达0.12%。这一结论从理论上分析，当亚表面缺陷绝对深度减小到百微米量级时，亚表

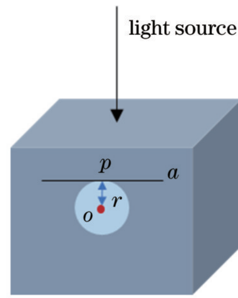

图 11　TSOM 扫描缺陷光强最大位置示意图

Fig. 11　Schematic diagram of maximum position of light intensity of TSOM scanning defect

表 2　增加半径大小后的缺陷深度

Table 2　Depth of defect after increasing radius size

Number of scans	Defect depth / μm	Number of scans	Defect depth / μm
1	1996. 1	9	1996. 1
2	1999. 1	10	2002. 0
3	2000. 1	11	1999. 1
4	2000. 5	12	1997. 6
5	2000. 5	13	2002. 0
6	2001. 3	14	2003. 5
7	1999. 8	15	2004. 9
8	2002. 0	16	2000. 5

面缺陷定位标准差仅为亚微米量级。经过实验发现，玻璃 3D 刻蚀微加工的方法可用于加工实验所需深度的亚表面缺陷。在使用 TSOM 定位微米量级亚表面缺陷深度时，需对折射率进行补偿矫正，进一步提高亚表面缺陷的深度定位精度。当亚表面缺陷尺寸较大时，仿真和实验一致表明，TSOM 的散射光强分布受缺陷自身体积影响，即存在体积效应，对定位微米量级缺陷中心到表面的深度具有重要影响。经过实验发现，本方法在扫描时，样品移动一个步长静止后才进行采图，降低了测量速度，后续也会进一步深入研究，提高检测速度。

参 考 文 献

[1] 陈明君，王会尧，程健，等．熔石英光学元件加工亚表面缺陷检测及抑制技术研究进展[J]. 机械工程学报，2021，57(20)：1-19.
Chen M J, Wang H Y, Cheng J, et al. Progress in detection and suppression techniques for processing-induced sub-surface defects of fused silica optical elements[J]. Journal of Mechanical Engineering, 2021, 57(20): 1-19.

[2] Chen C, Sun A Y, Ju B F, et al. Width and depth gauging of rectangular subsurface defects based on all-optical laser-ultrasonic technology[J]. Applied Acoustics, 2022, 191: 108684.

[3] Zhao D F, Cui J N, Bian X Y. Overview of subsurface damage detection technologies for ultra-smooth quartz components[C]//2021 IEEE 15th International Conference on Electronic Measurement & Instruments (ICEMI), October 29-31, 2021, Nanjing, China. New York: IEEE Press, 2022: 364-369.

[4] Dwivedi S K, Vishwakarma M, Soni P A. Advances and researches on non destructive testing: a review[J]. Materials Today: Proceedings, 2018, 5(2): 3690-3698.

[5] 邱啸天．基于量子点标记的光学元件亚表面缺陷检测技术[D]. 西安：西安工业大学，2021：1-5.
Qiu X T. Subsurface defect detection technology of optical components based on quantum dot marking[D]. Xi′an: Xi′an Technological University, 2021: 1-5.

[6] 张健浦，孙焕宇，王狮凌，等．熔融石英光学元件亚表面缺陷三维重构技术[J]. 光学学报，2020，40(2)：0216001.
Zhang J P, Sun H Y, Wang S L, et al. Three-dimensional reconstruction technology of subsurface defects in fused silica optical components[J]. Acta Optica Sinica, 2020, 40(2): 0216001.

[7] 张健浦．熔石英光学元件亚表面/体缺陷检测关键技术研究[D]. 杭州：浙江大学，2020：1-10.
Zhang J P. Research on key technologies of subsurface/body defect detection of fused quartz optical elements[D]. Hangzhou: Zhejiang University, 2020: 1-10.

[8] 胡陈林，毕果，叶卉，等．光学元件磨削加工亚表面损伤检测研究[J]. 人工晶体学报，2014，43(11)：2929-2934.
Hu C L, Bi G, Ye H, et al. Research on detection of subsurface damage on grinding optical elements[J]. Journal of Synthetic Crystals, 2014, 43(11): 2929-2934.

[9] 王华林．基于全内反射法测量亚表面损伤深度位置的研究[D]. 南京：南京理工大学，2016：11-20.
Wang H L. Study on measuring the depth and position of subsurface damage based on total internal reflection method[D]. Nanjing: Nanjing University of Science and Technology, 2016: 11-20.

[10] 朱晓娟．亚表面损伤测量技术中全内反射粗定位系统的研究[D]. 南京：南京理工大学，2015.
Zhu X J. Research on total internal reflection coarse positioning system in subsurface damage measurement technology[D]. Nanjing: Nanjing University of Science and Technology, 2015.

[11] Bashkansky M, Duncan M D, Kahn M, et al. Subsurface defect detection in ceramics by high-speed high-resolution optical coherent tomography[J]. Optics Letters, 1997, 22(1): 61-63.

[12] 张运旭．频域光学相干层析术成像深度提高方法研究[D]. 南京：南京理工大学，2017：6-11.
Zhang Y X. Study on the method of improving the imaging depth of frequency domain optical coherence tomography[D]. Nanjing: Nanjing University of Science and Technology, 2017: 6-11.

[13] 王昌明，高万荣．基于微米 SDOCT 的玻璃亚表面缺陷散射系数测量[J]. 光学学报，2021，41(7)：0729001.
Wang C M, Gao W R. Measurement of scattering coefficient of glass subsurface defects based on micron SDOCT[J]. Acta Optica Sinica, 2021, 41(7): 0729001.

[14] 伍秀玭，高万荣，张运旭，等．非破坏性玻璃亚表面缺陷定量检测新方法[J]. 中国激光，2017，44(6)：0603001.
Wu X P, Gao W R, Zhang Y X, et al. New method for non-destructive quantitative measurement of subsurface damage within glasses[J]. Chinese Journal of Lasers, 2017, 44(6): 0603001.

[15] Sindel J, Petschelt A, Grellner F, et al. Evaluation of subsurface damage in CAD/CAM machined dental ceramics[J]. Journal of Materials Science: Materials in Medicine, 1998, 9(5): 291-295.

[16] Lee J H, Na S, Jeong J, et al. Comparative near infrared through-focus scanning optical microscopy for 3D memory subsurface defect detection and classification[J]. Proceedings of SPIE, 2021, 11611: 116110T.

[17] Nie H T, Peng R J, Ren J J, et al. A through-focus scanning optical microscopy dimensional measurement method based on deep-learning classification model[J]. Journal of Microscopy, 2021, 283(2): 117-126.

[18] Zhang Z G, Ren J J, Peng R J, et al. Focused and TSOM images two-input deep-learning method for through-focus

scanning measuring[J]. Applied Sciences, 2022, 12(7): 3430.

[19] Qu Y F, Ren J J, Peng R J, et al. Imaging error compensation method for through-focus scanning optical microscopy images based on deep learning[J]. Journal of Microscopy, 2021, 283(2): 93-101.

[20] Rim M H, Agocs E, Dixson R, et al. Detecting nanoscale contamination in semiconductor fabrication using through-focus scanning optical microscopy[J]. Journal of Vacuum Science & Technology B, 2020, 38(5): 050602.

[21] Ryabko M V, Koptyaev S N, Shcherbakov A V, et al. Method for optical inspection of nanoscale objects based upon analysis of their defocused images and features of its practical implementation[J]. Optics Express, 2013, 21(21): 24483-24489.

[22] Ayal G, Malkes E, Aharoni E, et al. Sensitivity of LWR and CD linearity to process conditions in active area[J]. Proceedings of SPIE, 2011, 7971: 79711Q.

[23] Zhu J L, Liu J M, Xu T L, et al. Optical wafer defect inspection at the 10 nm technology node and beyond[J]. International Journal of Extreme Manufacturing, 2022, 4(3): 032001.

Subsurface Defect Detection Method of Optical Elements Based on Through-Focus Scanning Optical Microscopy

Wang Na[1,2], Liu Lituo[2*], Song Xiaojiao[2], Wang Dezhao[2,3], Wang Shengyang[2,4], Li Guannan[2], Zhou Weihu[1,2,3,4**]

[1]*School of Instrument Science and Opto-electronics Engineering, Hefei University of Technology, Hefei* 230009, *Anhui, China*;

[2]*Optoelectronic Center, Institute of Microelectronics, Chinese Academy of Sciences, Beijing* 100029, *China*;

[3]*School of Optoelectronic Engineering, Changchun University of Science and Technology, Changchun* 130022, *Jilin, China*;

[4]*School of Instrumentation and Optoelectronic Engineering, Beihang University, Beijing* 100191, *China*

Abstract

Objective With the vigorous development of technology in optics and semiconductors, transparent devices with smooth surfaces such as high-precision optical glass are widely employed in semiconductor and other fields. During grinding and polishing, optical glass inevitably produces a large number of scratches, pockmarks, bubbles, pollution particles, microcracks, and other defects in the subsurface. Micron/nanoscale subsurface defects will reduce the physical properties of transparent samples such as optical components, and seriously affect the development of processing and manufacturing technologies in optics and semiconductors. How to detect the subsurface defects of transparent optical components with high precision and provide key parameters for the high-precision preparation of transparent optical components has become an urgent problem in optical inspection. Subsurface defect detection technologies include destructive and non-destructive ones. Destructive detection technologies are simple to operate, and can intuitively and effectively observe the detection results, but they will make the test defects and the actual defects different. Therefore, the existing subsurface defect detection methods mainly focus on non-destructive detection technologies, including total internal reflection microscopy (TIRM), optical coherence tomography (OCT), and laser confocal scanning microscopy (CLSM), but these detection technologies cannot take into account both resolution and detection speed. Through-focus scanning optical microscopy (TSOM) is a model-based optical computational imaging method that can achieve non-contact, non-destructive, and fast measurement of three-dimensional nanostructures. TSOM features high sensitivity, simple hardware system, and sensitivity to nanoscale size changes, and it is not limited by the optical diffraction limit and can conduct online detection. To quickly and non-destructively detect subsurface defects of transparent samples, we propose a new method for detecting micronscale defects in the subsurface of optical components by TSOM and explore it in detail.

Methods The incident light from the halogen lamp source is irradiated to the subsurface of the sample. Scattering occurs where a defect exists and the scattering light is imaged by the objective lens to the CCD target detector. This method is based on traditional light microscopy and equipped with a high-precision piezoelectric ceramic displacement stage to control the Z movement of the sample, with the movement positioning accuracy of 1 nm. A series of optical images of the subsurface defects are obtained at a certain range of defocus positions from above to below the focus point by scanning along the propagation direction of the light field (Z direction). The images series are stacked according to spatial positions to form an image cube (TSOM cube). Then, the image cube is sliced along the Z direction to generate the TSOM image. The TSOM image is processed through data analysis algorithms to obtain three-dimensional information such as size, shape, and position of micronscale and nanoscale structures, and the target is located by the maximum gray value.

Results and Discussions The method can be adopted to detect and locate micronscale defects (Fig. 5). As the refractive index of scattered light is different in different materials, compensation and correction of the refractive index are necessary to obtain the actual depth of the defects (Fig. 7). According to the refraction law, the compensation and correction formula for the refractive index can be derived [Eq. (1)]. After TSOM scanning, the actual depth of the subsurface defects can be calculated based on Eq. (1). Experimental comparison and simulation (Fig. 10) show that larger subsurface defects exhibit volume effects. The position of the maximum light intensity corresponding to the defect in TSOM scanning is point p at the intersection of the radius parallel to the optical axis and its tangent (Fig. 11). To accurately determine the depth from the sample surface to the center of the defect, we should add the defect radius to the depth calculated in the TSOM scanning. After the radius correction, the average depth of the defect is 2000.3 μm, with a standard deviation of 2.4 μm and a relative standard deviation of 0.12%. Compared with other measurement methods, the depth deviation is 1.8 μm (Table 2).

Conclusions The TSOM method can be employed to detect micronscale subsurface defects in transparent glass and locate the defect depth with a relative standard deviation of up to 0.12%. Theoretically, when the absolute depth of subsurface defects is reduced to hundred-microns, the standard deviation of subsurface defect location is only sub-microns. When TSOM is utilized to locate the depth of subsurface defects at the micrometer scale, it is necessary to compensate and correct the refractive index to further improve the accuracy of defect depth location. When the size of the subsurface defect is large, both the simulation and experiment show that the scattering light intensity distribution of TSOM is affected by the volume effect of the defect itself, which has an important influence on the depth of locating the center of micronscale defects.

Key words subsurface defects; defect detection; through-focus scanning optical microscopy; depth positioning